Optics and Photonics Journal, **2012, 2, 119-122**
http://dx.doi.org/10.4236/opj.2012.22016 Published Online June 2012 (http://www.SciRP.org/journal/opj)

Extracavity Parametric Oscillation with Continuous and/or Discontinuous Frequency Tuning

Valerik S. Ayrapetyan, Tamara A. Shirokova
Siberian State Academy of Geodesy 10, Novosibirsk, Russia
Email: v.hayr100011@mail.ru

Received March 16, 2012; revised April 14, 2012; accepted April 23, 2012

ABSTRACT

A continuously or/and discontinuously tunable $LiNbO_3$ Optical Parametric Oscillator (OPO) with the spectral range of 1.42 - 4.24 um and shifting of 0…12 nm is created and investigated. The OPO resonator ring circuit provides for the radiation energy output value of up to 50 mJ. Radiation bandwidth narrowing of up to 0.7 cm^{-1} by introducing of the Fabry-Perot etalon into the OPO resonator has been obtained.

Keywords: Optical Parametric Oscillator; Fabry-Perot Etalon; Analog-Digital Converter

1. Introduction

Tunable laser optical sources with laser wavelength of 1.4 - 4.5 um are of great practical utility. In particular they are widely used to solve spectroscopy tasks in the field of atmosphere components remote sensing. Tunable lasers based on optical parametric oscillation with non-linear crystals are of greatest interest. Nd pulse lasers are conventionally used as a source of parametric oscillator pumping, while nonlinear crystals (NLC) $KNbO_3$, $LiNbO_3$, KTP, KTA, etc. [1] serve for frequency conversion. The principal OPO characteristics important for atmosphere remote sensing are low angular divergence combined with narrow spectral width and high OPO output performance.

At present the feature analysis of extra-cavity OPO with $LiNbO_3$ resulted in a quantity of optical schemes [2-7]. The study of basic linear networks of OPO cavities [3,4] has shown that at satisfactory energy indictors the oscillator's divergence angle is rather high and runs up at the pumping energy increase.

The implementation of OPO confocal unstable cavity [7,8] provides for high quality of output beam at a divergence angle that is close to a diffraction one. However, such cavities are extra sensitive to disalignment and are suitable only to provide oscillation at a stable wavelength. Basic research of OPO cavities [9] and their computer simulation [10] show that image-rotation cavities ensure high quality of the output beam.

Our experimental research findings [11] as well as some other works [6] prove that three-mirror ring OPO cavities provide for low beam divergence at high output performance.

The purpose of our study is to create a high performance OPO capable of continuous or/and discontinuous tuning of output wavelength within the range of 1.41 - 4.24 um. In order to provide for the above mentioned OPO output tuning types within the limits of the present study we chose a $LiNbO_3$ NLC with high non-linear and electrooptical factors. The choice of the three-mirror ring cavity is stipulated by the advantage of this optical scheme over the linear ones because it ensures parametrical oscillation in the travelling wave mode. The three-mirror cavity is less sensitive to disalignment. This cavity excludes stationary waves and has relatively homogeneous radiation intensity in comparison with linear cavities. The latter reason is of much importance because of low optical break-down of $LiNbO_3$ crystal (300 MW/cm^2). The three-mirror cavity rotates an image after each round trip. It compensates for inhomogeneity of the transverse structure of an OPO oscillated beam significantly, and diminishes the influence of optical inhomogeneities of $LiNbO_3$ crystal pumping beam.

2. Materials and Methods

For OPO pumping a laser with an active element YAG: Nd^{3+} of ∅6.3 × 100 mm is used. Pumping laser design is that of a telescopic unstable cavity. Radiation energy at the wavelength of λ = 1.064 um amounted to 180 mJ, and radiation pulse duration was 10 ns. Parametric conversion results in pulse duration of 8 ns at the total signal and idler waves, pulse energy of up to 50 mJ that is equal to ≈28% of the conversion efficiency. Optimal pulse frequency when the power differs slightly from the average power in low pulse frequency mode was at a level of

20 - 30 Hz. One should mention that at the increasing pulsed frequency (>30 Hz) considerable power instability (over 30%) occurs. This is connected with induced thermal lens effect and induced optical inhomogeneity (optical damage) effect in $LiNbO_3$ nonlinear crystal. The study is linear-polarized horizontally. Beam section intensity distribution has the appearance of concentric rings.

Figure 1 shows an optical scheme of a three-mirror ring OPO cavity having the shape of an equal triangle with the perimeter of 90 cm.

Active element (AE) from $LiNbO_3$ NLC of 10 × 10 × 30 mm is oriented at $\theta = 47$, $\varphi = -90$ NLC input pumping beam diameter is 6 mm. NLC is located on a rotating platform with a stepping motor (SM), rotating accuracy and step size are 3 arcsec and 0.03 cm^{-1} correspondingly. AE yaw movement provides for smooth OPO output wavelength tuning.

In case it is necessary to narrow the spectral bandwidth there is a Fabry-Perot etalon (FPE) of 500 um width on a rotating platform in OPO cavity. OPO spectral bandwidth narrowing in the whole frequency tuning range is achieved by synchronous rotation of AE and FPE. Scan time for the whole OPO tuning spectral bandwidth (1.41 - 1.85, 2.9 - 4.2 um) was equal to 5.2 s, while smooth tuning step size corresponded to 0.7 cm^{-1}. FPE influences directly the signal wave that narrows an idler wave automatically. FPE is placed into OPO part where there is no powerful pumping wave emission.

Discontinuous OPO tuning is performed by DC voltage supply to NLC nonworking surfaces with the voltage value specifying the discontinuous tuning step. In our study the maximum DC voltage value was equal to 4500 V. The value had to be changed at a step of 50 V that corresponds to the minimum OPO discontinuous tuning step of 0.133 nm. So, at the zero external field (E = 0) there is no discontinuous tuning, while at the external field voltage of U = 4500 V the maximum discontinuous tuning value is equal to 12 nm.

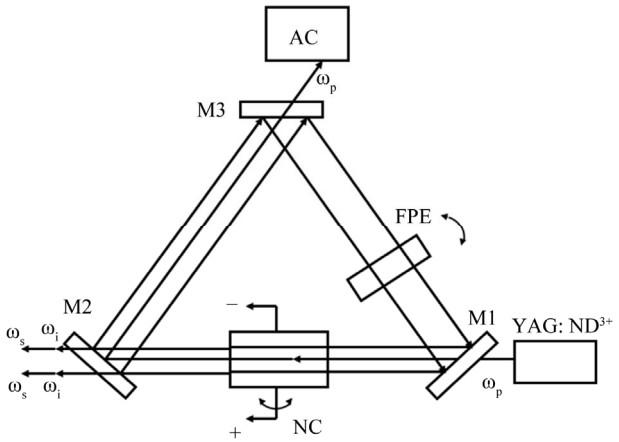

Figure 1. The scheme of a ring OPO cavity. YAG: Nd^{3+}—pumping laser; NC—nonlinear crystal $LiNbO_3$; M1, M2, M3—mirrors; FPE—Fabry-Perot Etalon; AC—pumping laser absorber cell; ω_s, ω_i, ω_p—signal and idler frequencies, and pumping laser frequency.

OPO wavelength shift at NCL heating is controlled and compensated by software to a tolerance of 0.1˚C.

Figure 2 shows an optical scheme of OPO bandwidth and wavelength measurement.

The definition of absolute value of the measured OPO wavelength (λ_{meas}) is performed by λ_{meas} correction method at a known gas absorption line or this purpose part of OPO emission (~3%) reflects from plane-parallel CaF_2-plate (3) and enters diffuse scattering sphere (8). Detector (5) receives stray radiation of the first channel after gas cell (7) with known gas (here methane 90%, at the pressure of 1 atm). Simultaneously the similar detector (5) receives stray radiation of the second channel. Then the electric signals run from the detectors to two inputs of ADC (4) which is connected to PC (10). The PC display shows a vibration rotation absorption spectrum υ_3 of the methane band, which central branch Q is a benchmark. Specialized software processes the data received, correlates them with Q-branch and displays the true value of OPO wavelength (λ_{meas}). For OPO wavelength calibration on the diffusing sphere there is a possibility to install IR-fibre (9) to transfer lasing to the entrance slit of monochromator MDR-12 (11).

OPO output energy was measured by calorimetric power meter S310 (USA).

3. Results and Discussion

The study of OPO power performance has been executed under extreme environment temperature conditions in the laboratory (T = +30˚C) and in the open air (T = –10˚C). Under the given conditions after 30 minutes of laser activity at a pulse frequency of 25 Hz the energy instability was within ±6%.

Figure 3 shows signal wavelength (λ = 1.42 - 1.75 um) and idler wavelength (λ = 2.9 - 4.2 um) dependence of OPO radiation energy.

An abrupt fall of the signal wave at 1.69 um and lack of idler wave oscillation at 2.85 are connected with heavy absorption of lithium niobate at 2.85 um. The implemented OPO scheme achieved the total conversion factor of 27%. The numerical value of beam angular divergence was calculated according to [9] as the relation of diaphragm diameter to the lens focus distance (d/l) with the diaphragm receiving 86% of total OPO pulse energy. Moreover the diaphragm was placed in the lens' plane.

While OPO oscillation is given as superposition of signal and idler waves, knowing the far field beam parameters helps to evaluate separate wave energy distribution

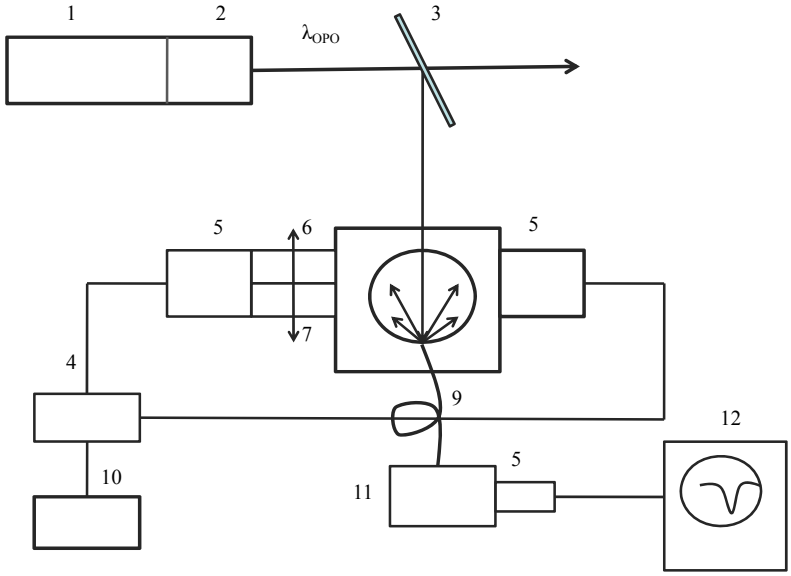

Figure 2. The optical scheme of OPO bandwidth and wavelength measurement. 1—pumping laser YAG:Nd^{3+}; 2—OPO unit; 3—CaF_2 plane-parallel plate; 4—analog-digital converter (ADC); 5—FD-219 photodetector with PbSe preamplifier; 6—methane cell; 7—gas cell; 8—diffusing sphere; 9—IR-fiber of CaF_2; 10—PC; 11—MDR-12 monochromator; 12—C1-91 os-cillograph.

character. Experimental OPO signal and idler wave divergence values were limited by 3.5 millirad within the whole oscillation range (**Figure 3**). At minor cavity length variation the value did not change significantly. The received result corresponded to the divergence calculation according to M^2 method [12]. **Figure 4** shows OPO emission spectra obtained for signal and idler waves.

Figure 4(a) corresponds to OPO emission spectrum without FPE in the cavity. **Figure 4(b)** shows the degree of OPO emission spectrum narrowing at FPE introduction. Similar spectra were received within the whole range of OPO tuning wavelengths. The narrowing of OPO emission spectrum half width varied from 4 to 5 times. Here the change of OPO emission power was insignificant.

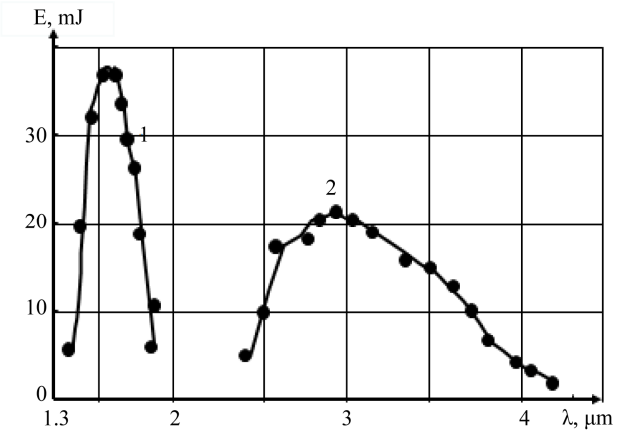

Figure 3. Distribution of OPO emission energy in signal and idler waves. 1—signal wave; 2—idler wave.

4. Conclusions

In conclusion some basic characteristics of IR OPO will be presented:

Continuous tuning area	1.42 - 1.85; 2.9 - 4.2 um
Discontinuous tuning value	0 - 12 nm
Total pulse energy	up to 50 mJ
Emission divergence	≤3.5 m rad
Spectral bandwidth	0.7 - 0.9 cm^{-1}
Pulse frequency	25 - 30 Hz
Pulse duration	10 ns

So, according to the study of non-linear optical characteristics of $LiNbO_3$ and KTP crystals, as well as on the

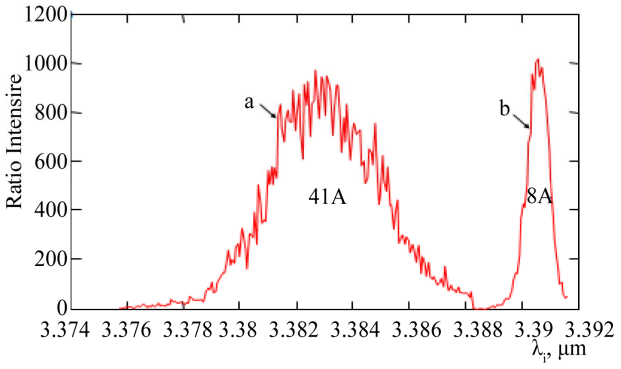

Figure 4. OPO idler wave emission spectra. (a) without FPE (λ_{01} = 3.383 um) $\Delta\nu$ = 3.6 cm^{-1}; (b) with FPE (λ_{02} = 3.391 um) $\Delta\nu_э$ = 0.69 cm^{-1}.

basis of up-to-date engineering and software developments an IR OPO with continuous and/or discontinuous frequency tuning has been created and tested. Thanks to its characteristics the present IR OPO can be used both in lidar units and at solving of various spectroscopy tasks of fundamental research.

REFERENCES

[1] V. G. Dmitriev, G. G. Gurzadyan and D. N. Nikogosyan, "Handbook of Nonlinear Optical Crystals," 2nd Edition, *Springer Series in Optical Sciences*, Vol. 64, 1999.

[2] M. D. Ewbank, M. J. Rosker and G. L. Bennett, "Frequency Tuning a Mid-Infrared Optical Parametric Oscillator by the Electro-Optic Effect," *Journal of the Optical Society of America*, Vol. 14, No. 3, 1997, pp. 663-668. doi:10.1364/JOSAB.14.000666

[3] A. V. Smith, W. J. Alford, T. D. Raymond and M. S. Bowers, "Comparison of Numerical Model with Measured Performance of a Seeded Nanosecond KTP Optical Parametric Oscillator," *Journal of the Optical Society of America*, Vol. 12, No. 11, 1995, p. 2253. doi:10.1364/JOSAB.12.002253

[4] L. R. Marshal, A. D. Hay and R. Burnham. Tech. Dig. Papers Adv. CLEO'90 Post Deadline Paper CDPO 35-1, 1990.

[5] A. H. Harutjunyan, G. A. Papyan, S. S. Sargsyan and T. K. Sargsyan, "High Efficiency Intricately Optical Parametric Oscillator Based on a Litium Niobate Cristal," *Proceedings of the International Conference of the ICONO*'91, *I*, *PWH*12, Leningrad, 24-27 September 1991, pp. 163-167.

[6] V. L. Naumov, A. M. Onishchenko, A. S. Podstavkin and A. V. Shestakov, "Extracavity Optical Parametric Oscillation at λ = 1.5 and 2 um and YAG Laser Pumping: Nd^{3+}," *Quantum Electronic*, Vol. 32, No. 3, 2002, pp. 225-228. doi:10.1070/QE2002v032n03ABEH002167

[7] A. I. Vodchits, V. I. Dashkevich, N. S. Kazak, V. K. Pavlenko, V. I. Pokryshkin, I. P. Petrovich, V. V. Rukhovets, A. S. Kraskovskiy and V. A. Orlovich, "Eye-Safe Emitter on the Basis of Optical Parametric Oscillator," *Journal of Applied Spectroscopy*, Vol. 73, No. 2, 2006, pp. 255-259. doi:10.1007/s10812-006-0070-8

[8] M. K. Brown and M. S. Bowers, "High Energy Near Diffraction Limited Output from Optical Parametric Oscillators Using Unstable Resonators," *Solid State Laser VI*, 10-11 February, San Jose, California, Vol. 2986, 1997, pp. 113-122.

[9] Y. A. Ananyev, "Optical Cavities and Laser Beams," Nauka, Moscow, 1990, p. 211.

[10] A. V. Smith and M. S. Bowers, "Image-Rotating Cavity Designs for Improved Beam Quality in Nanosecond Optical Parametric Oscillators," *Journal of the Optical Society of America*, Vol. 18, No. 5, 2001, pp. 701-706. doi:10.1364/JOSAB.18.000706

[11] V. S. Hayrapetyan, G. M. Apresyan, K. A Sargsyan and T. K. Sargsyan "Tunable OPO for Differential Absorption LIDAR's," *Abstract of International Quantum Electronic Conference* (*IQEC*) *and the Conference on Lasers*, *Applications*, *and Technologies* (*LAT*), *LMI* 72, Moscow, 22-28 June 2002, pp. 87-89.

[12] N. Hodgson and H. Weber, "Optical Resonator: Fundamentals, Advanced, Concepts and Application," 2*nd* Edition, Springer, London, 1997, p. 226.

